

Weierstraß-Institut für Angewandte Analysis und Stochastik

im Forschungsverbund Berlin e. V.

Preprint

ISSN 0946 – 8633

Stable computing with an enhanced physics based scheme for the 3d Navier-Stokes equations

M. A. Case¹, V. J. Ervin², A. Linke³, L. G. Rebholz⁴, N. E. Wilson⁵

submitted: April 22, 2010

¹ Clemson University
email: mcase@clemson.edu

² Clemson University
email: vjervin@clemson.edu

³ Weierstrass Institute for Applied Analysis and Stochastics
email: linke@wias-berlin.de

⁴ Clemson University
email: rebholz@clemson.edu

⁵ Clemson University
email: newilso@clemson.edu

No. 1509
Berlin 2010



2010 *Mathematics Subject Classification.* 76D05 65M60.

Key words and phrases. incompressible Navier-Stokes equations, finite element methods, grad-div stabilization, helicity conservation.

M. Case, L. Rebholz, and N. Wilson partially supported by National Science Foundation grant DMS0914478.

V. Ervin partially supported by the US Army Research Office under grant W911NF-05-1-0380.

Edited by
Weierstraß-Institut für Angewandte Analysis und Stochastik (WIAS)
Mohrenstraße 39
10117 Berlin
Germany

Fax: +49 30 2044975
E-Mail: preprint@wias-berlin.de
World Wide Web: <http://www.wias-berlin.de/>

Abstract

We study extensions of the energy and helicity preserving scheme for the 3D Navier-Stokes equations, developed in [23], to a more general class of problems. The scheme is studied together with stabilizations of grad-div type in order to mitigate the effect of the Bernoulli pressure error on the velocity error. We prove stability, convergence, discuss conservation properties, and present numerical experiments that demonstrate the advantages of the scheme.

1 Introduction

This paper extends the methodology of the enhanced-physics based scheme for the 3D Navier-Stokes equations (NSE) proposed in [23] (defined in Section 2) from its original derivation for space-periodic problems to a more general class of problems. This scheme is referred to as *enhanced-physics* because it is the only scheme that conserves *both* discrete energy and discrete helicity for the full 3D NSE. The key ingredient for the dual conservation scheme is using the rotational form of the nonlinearity with a projected vorticity, which allows the discrete nonlinearity to preserve both of the quantities. Since the (continuous) NSE nonlinearity conserves both energy and helicity, and jointly cascades them from the large scales through the inertial range to small viscosity dominated scales [3, 5], if the discrete nonlinearity does not also conserve energy and helicity it will introduce numerical error into the cascade, and bring into question the physical relevance of computed approximations.

It is a widely held belief in computational fluid dynamics (CFD) that the more *physically correct* a numerical scheme is, the more accurate its predictions will be, especially over long time intervals. In systems of conservation laws for fluids there is typically a second integral invariant in addition to energy, and its accurate treatment in a numerical scheme generally produces more accurate simulations than do schemes that do not specifically conserve this quantity. Beginning with Arakawa's energy and enstrophy conserving scheme for the 2D NSE [1] and related extensions [8], to energy and potential enstrophy schemes pioneered by Arakawa and Lamb, and Navon, [2, 19, 20], and most recently to an energy and helicity conserving scheme for 3D axisymmetric flow by J.-G. Liu and W. Wang [16], enhanced physics based schemes have provided more accurate simulations, especially over longer time intervals.

The fundamental challenge in extending the scheme of [23] to non-periodic problems is to avoid the large errors often present when the rotational form of the nonlinearity and the Bernoulli pressure is used. In the usual a priori error analysis for the velocity

approximation for the NSE, a consequence that the discrete divergence free velocity is not exactly divergence free, is a pressure error contribution

$$\frac{C}{\nu} \inf_{q_h \in Q_h} \|p - q_h\| \quad (1.1)$$

where $\nu = 1/\text{Reynolds number}$ denotes the kinematic viscosity [9, 15]. For problems whose pressure gradients are small this term is often negligible. However, using the rotational form of the NSE, and introducing the Bernoulli pressure $p + \frac{1}{2}|u|^2$ can bring prominence to this term, since the gradient of the Bernoulli pressure may be large due to boundary layers in the velocity field.

Following recent work in [14, 17, 4], a natural way to mitigate the pressure's error influence on the velocity approximation is to introduce grad-div stabilization. As we show, this reduces the effect of the Bernoulli pressure error. In the interest of physical fidelity, we also introduce a modified grad-div stabilization having the same effect on the error, but with less impact on the energy balance. Computational results show a slight improvement when this altered stabilization is used instead of usual grad-div stabilization.

This paper is arranged as follows. Section 2 presents mathematical preliminaries and notation, and defines the scheme studied in the remainder of the article. Section 3 is a study of stability and conservation laws for the scheme, and Section 4 presents a rigorous convergence analysis. Section 5 shows a numerical example which clearly illustrates the advantage of the scheme. Concluding remarks are given in Section 6.

2 Mathematical Preliminaries

We assume that Ω denotes a polyhedral domain in \mathbb{R}^3 . The $L^2(\Omega)$ norm and inner product are denoted by $\|\cdot\|$ and (\cdot, \cdot) . Likewise, the $L^p(\Omega)$ norms and the Sobolev $W_p^k(\Omega)$ norms are denoted $\|\cdot\|_{L^p}$ and $\|\cdot\|_{W_p^k}$, respectively. For the semi-norm in $W_p^k(\Omega)$ we use $|\cdot|_{W_p^k}$. H^k is used to represent the Sobolev space $W_2^k(\Omega)$, and $\|\cdot\|_k$ denotes the norm in H^k . For functions $v(x, t)$ defined on the entire time interval $[0, T]$, we define ($1 \leq m < \infty$)

$$\|v\|_{\infty, k} := \text{ess sup}_{[0, T]} \|v(t, \cdot)\|_k, \text{ and } \|v\|_{m, k} := \left(\int_0^T \|v(t, \cdot)\|_k^m dt \right)^{1/m}.$$

For the analysis in this paper, we assume no slip (i.e. homogeneous Dirichlet) boundary conditions for velocity and therefore use as our velocity and pressure spaces

$$X := (H_0^1(\Omega))^d, \quad Q := L_0^2(\Omega),$$

where Q is denoting the *mean zero* subspace of $L^2(\Omega)$.

We use as the norm on X the H^1 seminorm which, because of the boundary condition, is a norm, i.e. for $v \in X$, $\|v\|_X := \|\nabla v\|$. We denote the dual space of X by X^* , with the norm $\|\cdot\|_{X^*}$. The space of divergence free functions is defined by

$$V := \{v \in X : (\nabla \cdot v, q) = 0 \quad \forall q \in Q\}.$$

We denote conforming velocity, pressure finite element spaces based on a regular tetrahedralization, \mathcal{T}_h , of Ω (with maximum tetrahedron diameter h) by

$$X_h \subset X, Q_h \subset Q.$$

We assume that X_h, Q_h satisfy the usual inf-sup condition necessary for the stability of the pressure, i.e.

$$\inf_{q_h \in Q_h} \sup_{v_h \in X_h} \frac{(q_h, \nabla \cdot v_h)}{\|q_h\| \|v_h\|_X}. \quad (2.1)$$

Specifically, we assume that (X_h, Q_h) is made of (P_k, P_{k-1}) , $k \geq 2$ velocity pressure elements. Thus we have, for a given regular tetrahedralization \mathcal{T}_h ,

$$\begin{aligned} X_h &:= \{v_h : v_h|_e \in P_k(e), \forall e \in \mathcal{T}_h, v_h \in [C^0(\overline{\Omega})]^3, v_h|_{\partial\Omega} = 0\}, \\ Q_h &:= \{q_h : q_h|_e \in P_{k-1}(e), \forall e \in \mathcal{T}_h, q_h \in C^0(\overline{\Omega}), q_h \in L_0^2(\Omega)\}. \end{aligned}$$

The discretely divergence free subspace of X_h is

$$V_h = \{v_h \in X_h : (\nabla \cdot v_h, q_h) = 0 \quad \forall q_h \in Q_h\}.$$

We also use a more general space for the discrete vorticity space. Even though the velocity satisfies homogeneous Dirichlet boundary conditions, it is believed to be inappropriate to enforce homogeneous Dirichlet boundary conditions for the vorticity. A more physically consistent boundary condition is instead a no-slip boundary condition *along* the boundary, and hence we define the space

$$W_h := \{v_h : v_h \in [C^0(\Omega)]^3, \forall e \in \mathcal{T}_h (v_h)|_e \in P_k(e), v_h \times n|_{\partial\Omega} = 0\} \supset X_h.$$

We use $t^n := n\Delta t$, and for both continuous and discrete functions of time

$$v^{n+\frac{1}{2}} := \frac{v((n+1)\Delta t) + v(n\Delta t)}{2}.$$

2.1 Enhanced-physics based numerical schemes

We study three variations of the enhanced-physics based scheme of [23] extended to homogeneous Dirichlet boundary conditions for velocity. The first is a direct extension of the scheme to homogeneous boundary conditions. The second scheme adds usual grad-div stabilization (see [22]), that is, it adds the term $\gamma(\nabla \cdot (u_h^{n+1} + u_h^n)/2, \nabla \cdot v_h)$ to a Crank-Nicolson scheme. This term is derived from adding the (identically zero) term $-\gamma\nabla(\nabla \cdot u)$ at the continuous level. Discretely, this term penalizes for lack of mass conservation, and is known to reduce the effect of the pressure error on the velocity error for large Reynolds number problems [14, 17, 22]. In finite element computations of rotational form models the (Bernoulli) pressure error tends to be the dominant error source because it is as complex as the velocity but is approximated with lower degree polynomials, and its effect on the velocity error is amplified by the Reynolds number.

The potential downside from using this stabilization is a change in the energy balance. However, in practice this tradeoff is worthwhile.

In the interest of physical fidelity to the energy balance, in the third scheme we introduce an alternative stabilization that provides the same effect on reducing the effect of the pressure error on the velocity error, but with minimal impact on the physical energy balance (Section 3). The added stabilization term arises by adding the (also identically zero) term $-\gamma\nabla(\nabla \cdot u_t)$ at the continuous level, leading to the term $\gamma\frac{1}{\Delta t}(\nabla \cdot (u_h^{n+1} - u_h^n), \nabla \cdot v_h)$ in the FEM formulation. The computational results (Section 5) from using this stabilization show an improvement in accuracy over the usual grad-div stabilization for our test problem. However, we note that for steady problems this term will not have a stabilizing effect since it will be trivially zero.

There has been recent work done to optimally choose the constant γ that scales the stabilization term. Herein, we simply choose $\gamma = 1$ in the computations, which the analysis suggests is an appropriate choice. However, one could also choose this parameter element-wise, which would lead to better results [21]. We leave optimal parameter choice for these schemes as an interesting topic of future study.

Algorithm 2.1 (Enhanced-physics based schemes for homogeneous Dirichlet boundary conditions). *Given a time step $\Delta t > 0$, finite end time $T := M\Delta t$, and initial velocity $u_h^0 \in V_h$, find $w_h^0 \in W_h$ and $\lambda_h^0 \in Q_h$ satisfying $\forall (\chi_h, r_h) \in (W_h, Q_h)$*

$$(w_h^0, \chi_h) + (\lambda_h^0, \nabla \cdot \chi_h) = (\nabla \times u_h^0, \chi_h), \quad (2.2)$$

$$(\nabla \cdot w_h^0, r_h) = 0. \quad (2.3)$$

Then for $n = 0, 2, \dots, M-1$, find $(u_h^{n+1}, w_h^{n+1}, p_h^{n+1}, \lambda_h^{n+1}) \in (X_h, W_h, Q_h, Q_h)$ satisfying $\forall (v_h, \chi_h, q_h, r_h) \in (X_h, W_h, Q_h, Q_h)$

$$\begin{aligned} & \left(\frac{u_h^{n+1} - u_h^n}{\Delta t}, v_h \right) + \text{STAB} - (p_h^{n+1}, \nabla \cdot v_h) \\ & + (w_h^{n+\frac{1}{2}} \times u_h^{n+\frac{1}{2}}, v_h) + \nu(\nabla u_h^{n+\frac{1}{2}}, \nabla v_h) = (f(t^{n+\frac{1}{2}}), v_h) \end{aligned} \quad (2.4)$$

$$(\nabla \cdot u_h^{n+1}, q_h) = 0 \quad (2.5)$$

$$(w_h^{n+\frac{1}{2}}, \chi_h) + (\lambda_h^{n+1}, \nabla \cdot \chi_h) = (\nabla \times u_h^{n+\frac{1}{2}}, \chi_h) \quad (2.6)$$

$$(\nabla \cdot w_h^{n+\frac{1}{2}}, r_h) = 0. \quad (2.7)$$

where

$$\text{STAB} = \begin{cases} 0 & \text{Scheme 1} \\ \gamma(\nabla \cdot u_h^{n+\frac{1}{2}}, \nabla \cdot v_h) & \text{Scheme 2} \\ \frac{\gamma}{\Delta t}(\nabla \cdot (u_h^{n+1} - u_h^n), \nabla \cdot v_h) & \text{Scheme 3} \end{cases}$$

Remark 2.1. *We have found it computationally advantageous to decouple the 4 equation system (2.4)-(2.7) into a velocity-pressure system (2.4)-(2.5) and a projection system (2.6)-(2.7), then solve (2.4)-(2.7) by iterating between the two sub-systems. This typically requires more iterations and linear solves to converge than solving the fully-coupled system using a Newton method. However the linear solves are much easier*

in the decoupled system. Note also that for the decoupled system the work required is only slightly more than a usual implicit Crank-Nicolson method (i.e. without vorticity projection) since the extra work is (relatively inexpensive) projection solves. Moreover, for nonhomogeneous boundary conditions, this decoupling leads to a simplified boundary condition for the vorticity: $w_h = I_h(\nabla \times u_h)$ on the boundary, where I_h is an appropriate interpolation operator.

3 Stability, conservation laws, and existence of solutions

In this section we prove fundamental mathematical and physical properties of the 3 schemes: unconditional stability, solution existence and conservation laws. We begin with stability.

Lemma 3.1. *Solutions to Algorithm 2.1 are nonlinearly stable. That is, they satisfy:*
Scheme 1:

$$\|u_h^M\|^2 + \nu \Delta t \sum_{n=0}^{M-1} \left\| \nabla u_h^{n+\frac{1}{2}} \right\|^2 \leq \frac{\Delta t}{\nu} \sum_{n=0}^{M-1} \|f\|_*^2 + \|u_h^0\|^2 = C(data). \quad (3.1)$$

Scheme 2:

$$\|u_h^M\|^2 + \Delta t \sum_{n=0}^{M-1} \left(2\gamma \left\| \nabla \cdot u_h^{n+\frac{1}{2}} \right\|^2 + \nu \left\| \nabla u_h^{n+\frac{1}{2}} \right\|^2 \right) \leq \frac{\Delta t}{\nu} \sum_{n=0}^{M-1} \|f\|_*^2 + \|u_h^0\|^2 = C(data). \quad (3.2)$$

Scheme 3:

$$\begin{aligned} \|u_h^M\|^2 + \gamma \|\nabla \cdot u_h^M\|^2 + \nu \Delta t \sum_{n=0}^{M-1} \left\| \nabla u_h^{n+\frac{1}{2}} \right\|^2 \\ \leq \frac{\Delta t}{\nu} \sum_{n=0}^{M-1} \|f\|_*^2 + \|u_h^0\|^2 + \gamma \|\nabla \cdot u_h^0\|^2 = C(data). \end{aligned} \quad (3.3)$$

Schemes 1,2,3:

$$\Delta t \sum_{n=0}^{M-1} \left\| w_h^{n+\frac{1}{2}} \right\|^2 \leq \Delta t \sum_{n=0}^{M-1} \left\| \nabla u_h^{n+\frac{1}{2}} \right\|^2 = C(data). \quad (3.4)$$

Schemes 1,2,3:

$$\Delta t \sum_{n=1}^M \left(\|p_h^n\|^2 + \|\lambda_h^n\|^2 \right) \leq C(data). \quad (3.5)$$

$C(data)$ is a constant dependent on T, ν, γ, f, u_h^0 and Ω .

Proof. To prove the bounds on velocity for each of the schemes, choose $v_h = u_h^{n+\frac{1}{2}}$ in (2.4). The nonlinear and pressure terms are then zero. The triangle inequality, and summing over time steps then completes the proofs of (3.1),(3.2),(3.3).

To prove (3.4) choose $\chi_h = w_h^{n+\frac{1}{2}}$ in (2.6) and $r_h = \lambda_h^{n+1}$ in (2.7). After combining the equations we obtain

$$\begin{aligned} \left\| w_h^{n+\frac{1}{2}} \right\|^2 &= (\nabla \times u_h^{n+\frac{1}{2}}, w_h^{n+\frac{1}{2}}) \leq \left\| \nabla \times u_h^{n+\frac{1}{2}} \right\| \left\| w_h^{n+\frac{1}{2}} \right\| \\ &\leq \frac{1}{2} \left\| \nabla \times u_h^{n+\frac{1}{2}} \right\|^2 + \frac{1}{2} \left\| w_h^{n+\frac{1}{2}} \right\|^2 \leq \left\| \nabla u_h^{n+\frac{1}{2}} \right\|^2 + \frac{1}{2} \left\| w_h^{n+\frac{1}{2}} \right\|^2. \end{aligned}$$

Rearranging, and summing over time steps we obtain (3.4).

To obtain the stated bound for λ_h^n , we begin with the inf-sup condition satisfied by $X_h(\subset W_h)$ and Q_h and use (2.6) to obtain

$$\begin{aligned} \|\lambda_h^n\| &\leq \frac{1}{\beta} \sup_{\chi_h \in X_h} \frac{(\lambda_h^n, \nabla \cdot \chi_h)}{\|\chi_h\|_X} \leq \frac{1}{\beta} \sup_{\chi_h \in X_h} \frac{(\nabla \times u_h^{n-\frac{1}{2}}, \chi_h) - (w_h^{n-\frac{1}{2}}, \chi_h)}{\|\chi_h\|_X} \\ &\leq \frac{1}{\beta} \left(\|\nabla \times u_h^{n-\frac{1}{2}}\| + \|w_h^{n-\frac{1}{2}}\| \right) \leq \frac{2}{\beta} \left(\|\nabla u_h^{n-\frac{1}{2}}\| + \|w_h^{n-\frac{1}{2}}\| \right). \end{aligned}$$

Using the bounds for $\nabla u_h^{n+\frac{1}{2}}$ (see (3.1)-(3.3)) and $w_h^{n+\frac{1}{2}}$ (see (3.4)) we obtain the bound for λ_h^n . The bound for the pressure is established in an analogous manner. \square

Lemma 3.2. *Solutions exist to each of the three schemes presented in Algorithm 2.1.*

Proof. For each of the schemes, this is a straight-forward extension of the existence proof given for the periodic case in [23]. The result is a consequence of the Leray-Schauder fixed point theorem, and the stability bounds of Lemma 3.1. \square

We now study the conservation laws for energy and helicity in the schemes. It is shown in [23] that, when restricted to the periodic case, the non-stabilized scheme of Algorithm 2.1 (Scheme 1) conserves energy and helicity. In the case of homogeneous boundary conditions for velocity, this physically important feature for energy is still preserved. However, as one might expect, the stabilization terms in Schemes 2 and 3 alter the energy balance. Lemma 3.3 shows these energy balances.

The energy balance of Scheme 1, the unstabilized scheme, is analogous to that for the continuous NSE. However, for Scheme 2, we see the effect of the stabilization on the energy balance in the term $\gamma \Delta t \sum_{n=0}^{M-1} \left\| \nabla \cdot u_h^{n+\frac{1}{2}} \right\|^2$ on the left hand side of (3.7). For most choices of elements, one may have that each term in this sum is small, but over a long time interval this sum can grow to significantly (and non-physically) alter the balance. The energy balance for Scheme 3 differs from Scheme 1's energy balance in the addition of only two small terms, instead of a sum. Hence this indicates that the modified grad-div stabilization, for problems over a long time interval, offers a more physically relevant energy balance than the usual grad-div stabilization (Scheme 2).

Lemma 3.3. *The schemes of Algorithm 2.1 admit the following energy conservation laws.*

Scheme 1:

$$\frac{1}{2} \|u_h^M\|^2 + \nu \Delta t \sum_{n=0}^{M-1} \left\| \nabla u_h^{n+\frac{1}{2}} \right\|^2 = \Delta t \sum_{n=0}^{M-1} (f(t^{n+\frac{1}{2}}), u_h^{n+\frac{1}{2}}) + \frac{1}{2} \|u_h^0\|^2. \quad (3.6)$$

Scheme 2:

$$\frac{1}{2} \|u_h^M\|^2 + \nu \Delta t \sum_{n=0}^{M-1} \left\| \nabla u_h^{n+\frac{1}{2}} \right\|^2 + \gamma \Delta t \sum_{n=0}^{M-1} \left\| \nabla \cdot u_h^{n+\frac{1}{2}} \right\|^2 = \Delta t \sum_{n=0}^{M-1} (f(t^{n+\frac{1}{2}}), u_h^{n+\frac{1}{2}}) + \frac{1}{2} \|u_h^0\|^2. \quad (3.7)$$

Scheme 3:

$$\begin{aligned} \frac{1}{2} (\|u_h^M\|^2 + \gamma \|\nabla \cdot u_h^M\|^2) + \nu \Delta t \sum_{n=0}^{M-1} \left\| \nabla u_h^{n+\frac{1}{2}} \right\|^2 &= \Delta t \sum_{n=0}^{M-1} (f(t^{n+\frac{1}{2}}), u_h^{n+\frac{1}{2}}) \\ &+ \frac{1}{2} (\|u_h^0\|^2 + \gamma \|\nabla \cdot u_h^0\|^2). \end{aligned} \quad (3.8)$$

Proof. The proofs of these results follow from choosing $v_h = u_h^{n+\frac{1}{2}}$ in Algorithm 2.1 for each of the schemes. The key point is that the nonlinear term vanishes with this choice of test function, and thus does not contribute to the energy balance equations. \square

We now consider the discrete helicity conservation in Algorithm 2.1. We begin with the case of imposing Dirichlet boundary conditions on the projected vorticity, i.e. $W_h = X_h$. Although this case is nonphysical, analysis of it is the first step in understanding more complex boundary conditions.

In this case, the schemes' discrete nonlinearity preserves helicity, however the stabilization terms do not. We state the precise results in the next lemma. Denote the discrete helicity at time level n by $H_h^n := (u_h^n, \nabla \times u_h^n)$. Note that from (2.5),(2.6), $H_h^n := (u_h^n, w_h^n)$.

Lemma 3.4. *If $W_h := X_h$, the schemes of Algorithm 2.1 admit the following helicity conservation laws.*

Scheme 1:

$$H_h^M + 2\nu \Delta t \sum_{n=0}^{M-1} (\nabla u_h^{n+\frac{1}{2}}, \nabla w_h^{n+\frac{1}{2}}) = 2\nu \Delta t \sum_{n=0}^{M-1} (f(t^{n+\frac{1}{2}}), \nabla w_h^{n+\frac{1}{2}}) + H_h^0. \quad (3.9)$$

Scheme 2:

$$\begin{aligned} H_h^M + 2\nu \Delta t \sum_{n=0}^{M-1} (\nabla u_h^{n+\frac{1}{2}}, \nabla w_h^{n+\frac{1}{2}}) + 2\gamma \Delta t \sum_{n=0}^{M-1} (\nabla \cdot u_h^{n+\frac{1}{2}}, \nabla \cdot w_h^{n+\frac{1}{2}}) \\ = 2\Delta t \sum_{n=0}^{M-1} (f(t^{n+\frac{1}{2}}), \nabla w_h^{n+\frac{1}{2}}) + H_h^0. \end{aligned} \quad (3.10)$$

Scheme 3:

$$\begin{aligned}
H_h^M + 2\nu\Delta t \sum_{n=0}^{M-1} (\nabla u_h^{n+\frac{1}{2}}, \nabla w_h^{n+\frac{1}{2}}) + 2\gamma \sum_{n=0}^{M-1} (\nabla \cdot (u_h^{n+1} - u_h^n), \nabla \cdot w_h^{n+\frac{1}{2}}) \\
= 2\Delta t \sum_{n=0}^{M-1} (f(t^{n+\frac{1}{2}}), \nabla w_h^{n+\frac{1}{2}}) + H_h^0. \quad (3.11)
\end{aligned}$$

Proof. Choosing $v_h = w_h^{n+\frac{1}{2}}$ eliminates the nonlinear term and the pressure term from (2.4) for each of the 3 schemes, and reduces the time difference term to

$$\begin{aligned}
\frac{1}{\Delta t} (u_h^{n+1} - u_h^n, w_h^{n+\frac{1}{2}}) &= \frac{1}{\Delta t} (u_h^{n+1} - u_h^n, \nabla \times u_h^{n+\frac{1}{2}}) \\
= \frac{1}{2\Delta t} ((u_h^{n+1}, \nabla \times u_h^{n+1}) &+ (u_h^{n+1}, \nabla \times u_h^n) - (u_h^n, \nabla \times u_h^{n+1}) - (u_h^n, \nabla \times u_h^n)) \\
&= \frac{1}{2\Delta t} (H_h^{n+1} - H_h^n), \quad (3.12)
\end{aligned}$$

as, for $v, w \in H_0^1(\Omega)$, $(v, \nabla \times w) = (w, \nabla \times v)$.

Using (3.12) Scheme 1 becomes,

$$\frac{1}{2\Delta t} (H_h^{n+1} - H_h^n) + \nu(\nabla u_h^{n+\frac{1}{2}}, \nabla w_h^{n+\frac{1}{2}}) = (f(t^{n+\frac{1}{2}}), w_h^{n+\frac{1}{2}}) \quad (3.13)$$

Multiplying by $2\Delta t$ and summing over time steps completes the proof of (3.9).

The proofs of (3.10) and (3.11) follow the same way, except they will contain their respective stabilization terms. \square

Lemma 3.4 shows that if we impose Dirichlet boundary conditions on the vorticity, then the nonlinearity is able to preserve helicity. Hence for Scheme 1, we see a helicity balance analogous to that of the true physics. However, the stabilization terms do not preserve helicity, and thus appear in the helicity balances for Schemes 2 and 3.

Interestingly, if the term $\gamma(\nabla \cdot w_h^{n+1}, \nabla \cdot \chi_h)$ is added to the left hand side of the vorticity projection equation (2.6), one can show that Scheme 3 conserves both helicity and energy. This results from the cancellation of the stabilization term in Scheme 3's momentum equation when v_h is chosen to be $w_h^{n+\frac{1}{2}}$ and χ_h is chosen as u_h^{n+1} and u_h^n respectively. However, computations using this additional term with Scheme 3 were inferior to those of Scheme 3 defined above.

Similar conservation laws for helicity, even for Scheme 1, do not appear to hold for the nonhomogeneous boundary condition for vorticity, i.e. $X_h \neq W_h$. Due to the definitions of these spaces, extra terms arise in the balance that correspond to the difference between the projection of the curl into discretely divergence-free subspaces of W_h and X_h . These extra terms will be small except at strips along the boundary, but nonetheless global helicity conservation will fail to hold. However, more typical schemes, e.g. usual trapezoidal convective form or rotational form [13], introduce nonphysical helicity over the entire domain and thus the schemes of Algorithm 2.1 still provide a better treatment of helicity than such schemes.

4 Convergence

Three numerical schemes are described in Algorithm 2.1. We prove in detail convergence of solutions of Scheme 3 to an NSE solution. Convergence results for Schemes 1 and 2 can be established in an analogous manner.

We define the following additional norms:

$$\begin{aligned} \|v\|_{\infty,k} &:= \max_{0 \leq n \leq M} \|v^n\|_k, & \|v_{1/2}\|_{\infty,k} &:= \max_{1 \leq n \leq M} \|v^{n-1/2}\|_k, \\ \|v\|_{m,k} &:= \left(\sum_{n=0}^M \|v^n\|_k^m \Delta t \right)^{1/m}, & \|v_{1/2}\|_{m,k} &:= \left(\sum_{n=1}^M \|v^{n-1/2}\|_k^m \Delta t \right)^{1/m}. \end{aligned}$$

We also let $P_{V_h} : L^2 \rightarrow V_h$ denote the projection of L^2 onto V_h , i.e. $P_{V_h}(w) := s_h$ where

$$(s_h, v_h) = (w, v_h), \forall v_h \in V_h.$$

For simplicity in stating the a priori theorem we summarize here the regularity assumptions for the solution $u(x, t)$ to the NSE.

$$u \in L^2(0, T; H^{k+1}(\Omega)) \cap L^\infty(0, T; H^1(\Omega)), \quad (4.1)$$

$$u(\cdot, t) \in H_0^1(\Omega), \quad \nabla \times u \in L^2(0, T; H^{k+1}(\Omega)), \quad (4.2)$$

$$u_t \in L^2(0, T; H^{k+1}(\Omega)) \cap L^\infty(0, T; H^{k+1}(\Omega)), \quad (4.3)$$

$$u_{tt} \in L^2(0, T; H^{k+1}(\Omega)), \quad (4.4)$$

$$u_{ttt} \in L^2(0, T; L^2(\Omega)) \quad (4.5)$$

$$(u \times (\nabla \times u))_{tt} \in L^2(0, T; L^2(\Omega)). \quad (4.6)$$

Theorem 4.1. *For u, p solutions of the NSE with $p \in L^2(0, T; H^k(\Omega))$, u satisfying (4.1)-(4.6), $f \in L^2(0, T; X^*(\Omega))$, and $u_0 \in V_h$, (u_h^n, w_h^n) given by Scheme 3 of Algorithm 2.1 for $n = 1, \dots, M$ and Δt sufficiently small, we have that*

$$\begin{aligned} & \|u(T) - u_h^M\| + \|\nabla \cdot (u(T) - u_h^M)\| + \left(v \Delta t \sum_{n=0}^{M-1} \left\| \nabla (u^{n+\frac{1}{2}} - u_h^{n+\frac{1}{2}}) \right\|^2 \right)^{1/2} \leq \\ & C(\gamma, T, v^{-3}, u) \left(h^k \|u(T)\|_{k+1} + h^k \|u\|_{2,k+1} + h^k \|p\|_{2,k} + h^k \|u_t\|_{2,k+1} \right. \\ & + h^k \|u_t\|_{\infty,k+1} + h^k \|u_t\|_{\infty,1} \|u\|_{2,k+1} + (\Delta t)^{1/2} h^k \|u_{tt}\|_{2,k+1} + (\Delta t)^2 \|u_{ttt}\|_{2,0} \\ & \left. + (\Delta t)^2 \|u_{tt}\|_{2,1} + (\Delta t)^2 \|(u \times (\nabla \times u))_{tt}\|_{2,0} + h^{k+1} \|u\|_{\infty,1} \|\nabla \times u\|_{2,k+1} \right) \quad (4.7) \end{aligned}$$

Proof of Theorem. Since (u, p) solves the NSE, we have $\forall v_h \in X_h$ that

$$\begin{aligned} & (u_t(t^{n+\frac{1}{2}}), v_h) - (u(t^{n+\frac{1}{2}}) \times (\nabla \times u(t^{n+\frac{1}{2}})), v_h) - (p(t^{n+\frac{1}{2}}), \nabla \cdot v_h) \\ & + v(\nabla u(t^{n+\frac{1}{2}}), \nabla v_h) = (f(t^{n+\frac{1}{2}}), v_h). \quad (4.8) \end{aligned}$$

Adding $(\frac{u^{n+1}-u^n}{\Delta t}, v_h)$ and $v(\nabla u^{n+\frac{1}{2}}, \nabla v_h)$ to both sides of (4.8) we obtain

$$\begin{aligned} & \frac{1}{\Delta t}(u^{n+1} - u^n, v_h) + \left((\nabla \times u(t^{n+\frac{1}{2}})) \times u(t^{n+\frac{1}{2}}), v_h \right) - (p(t^{n+\frac{1}{2}}), \nabla \cdot v_h) + v(\nabla u^{n+\frac{1}{2}}, \nabla v_h) \\ &= (f(t^{n+\frac{1}{2}}), v_h) + \left(\frac{u^{n+1} - u^n}{\Delta t} - u_t(t^{n+\frac{1}{2}}), v_h \right) + v(\nabla u^{n+\frac{1}{2}} - \nabla u(t^{n+\frac{1}{2}}), \nabla v_h). \end{aligned} \quad (4.9)$$

Next, subtracting (2.4) from (4.9), label $e^n := u^n - u_h^n$, and adding the identically zero term $\gamma(\nabla \cdot (\frac{u^{n+1}-u^n}{\Delta t}), \nabla \cdot v_h)$ to the LHS gives

$$\begin{aligned} & \frac{1}{\Delta t}(e^{n+1} - e^n, v_h) + v(\nabla e^{n+\frac{1}{2}}, \nabla v_h) + \frac{\gamma}{\Delta t}(\nabla \cdot (e^{n+1} - e^n), \nabla \cdot v_h) \\ &= - \left(\nabla \times u(t^{n+\frac{1}{2}}) \times u(t^{n+\frac{1}{2}}), v_h \right) + \left(w_h^{n+\frac{1}{2}} \times u_h^{n+\frac{1}{2}}, v_h \right) + \left(p(t^{n+\frac{1}{2}}) - p_h^{n+1}, \nabla \cdot v_h \right) \\ & \quad + \left(\frac{u^{n+1} - u^n}{\Delta t} - u_t(t^{n+\frac{1}{2}}), v_h \right) + v \left(\nabla u^{n+\frac{1}{2}} - \nabla u(t^{n+\frac{1}{2}}), \nabla v_h \right). \end{aligned} \quad (4.10)$$

We split the error into two pieces Φ_h and η : $e^n = u^n - u_h^n = (u^n - U^n) + (U^n - u_h^n) := \eta^n + \Phi_h^n$, where U^n denotes the interpolant of u^n in V_h , yielding

$$\begin{aligned} & \frac{1}{\Delta t}(\Phi_h^{n+1} - \Phi_h^n, v_h) + v(\nabla \Phi_h^{n+\frac{1}{2}}, \nabla v_h) + \frac{\gamma}{\Delta t}(\nabla \cdot (\Phi_h^{n+1} - \Phi_h^n), \nabla \cdot v_h) = -\frac{1}{\Delta t}(\eta^{n+1} - \eta^n, v_h) \\ & \quad - v(\nabla \eta^{n+\frac{1}{2}}, \nabla v_h) - \frac{\gamma}{\Delta t}(\nabla \cdot (\eta^{n+1} - \eta^n), \nabla \cdot v_h) - \left((\nabla \times u(t^{n+\frac{1}{2}})) \times u(t^{n+\frac{1}{2}}), v_h \right) \\ & \quad + \left(w_h^{n+\frac{1}{2}} \times u_h^{n+\frac{1}{2}}, v_h \right) + (p(t^{n+\frac{1}{2}}) - p_h^{n+1}, \nabla \cdot v_h) + \left(\frac{u^{n+1} - u^n}{\Delta t} - u_t(t^{n+\frac{1}{2}}), v_h \right) \\ & \quad + v(\nabla u^{n+\frac{1}{2}} - \nabla u(t^{n+\frac{1}{2}}), \nabla v_h). \end{aligned} \quad (4.11)$$

Choosing $v_h = \Phi_h^{n+\frac{1}{2}}$ yields

$$\begin{aligned} & \frac{1}{2\Delta t} \left(\|\Phi_h^{n+1}\|^2 - \|\Phi_h^n\|^2 \right) + v \left\| \nabla \Phi_h^{n+\frac{1}{2}} \right\|^2 + \frac{\gamma}{2\Delta t} \left(\|\nabla \cdot \Phi_h^{n+1}\|^2 - \|\nabla \cdot \Phi_h^n\|^2 \right) \\ &= -\frac{1}{\Delta t}(\eta^{n+1} - \eta^n, \Phi_h^{n+\frac{1}{2}}) - v(\nabla \eta^{n+\frac{1}{2}}, \nabla \Phi_h^{n+\frac{1}{2}}) - \frac{\gamma}{\Delta t} \left(\nabla \cdot (\eta^{n+1} - \eta^n), \nabla \cdot \Phi_h^{n+\frac{1}{2}} \right) \\ & \quad - \left(\nabla \times u(t^{n+\frac{1}{2}}) \times u(t^{n+\frac{1}{2}}), \Phi_h^{n+\frac{1}{2}} \right) + \left(w_h^{n+\frac{1}{2}} \times u_h^{n+\frac{1}{2}}, \Phi_h^{n+\frac{1}{2}} \right) + (p(t^{n+\frac{1}{2}}) - p_h^{n+1}, \nabla \cdot \Phi_h^{n+\frac{1}{2}}) \\ & \quad + \left(\frac{u^{n+1} - u^n}{\Delta t} - u_t(t^{n+\frac{1}{2}}), \Phi_h^{n+\frac{1}{2}} \right) + v(\nabla u^{n+\frac{1}{2}} - \nabla u(t^{n+\frac{1}{2}}), \nabla \Phi_h^{n+\frac{1}{2}}). \end{aligned} \quad (4.12)$$

We have the following bounds for the terms on the RHS (see [6]).

$$-v(\nabla \eta^{n+\frac{1}{2}}, \nabla \Phi_h^{n+\frac{1}{2}}) \leq \frac{v}{12} \left\| \nabla \Phi_h^{n+\frac{1}{2}} \right\|^2 + 3v \left\| \nabla \eta^{n+\frac{1}{2}} \right\|^2 \quad (4.13)$$

$$\begin{aligned}
\frac{1}{\Delta t}(\eta^{n+1} - \eta^n, \Phi_h^{n+\frac{1}{2}}) &\leq \frac{1}{2} \left\| \frac{\eta^{n+1} - \eta^n}{\Delta t} \right\|^2 + \frac{1}{2} \left\| \Phi_h^{n+\frac{1}{2}} \right\|^2 \\
&= \frac{1}{2} \int_{\Omega} \left(\frac{1}{\Delta t} \int_{t^n}^{t^{n+1}} \eta_t dt \right)^2 d\Omega + \frac{1}{2} \left\| \Phi_h^{n+\frac{1}{2}} \right\|^2 \\
&\leq \frac{1}{2} \int_{\Omega} \left(2|\eta_t(t^{n+1})|^2 + 2 \int_{t^n}^{t^{n+1}} |\eta_{tt}|^2 dt \right) d\Omega + \frac{1}{2} \left\| \Phi_h^{n+\frac{1}{2}} \right\|^2 \\
&= \|\eta_t(t^{n+1})\|^2 + \int_{t^n}^{t^{n+1}} \|\eta_{tt}\|^2 dt + \frac{1}{2} \left\| \Phi_h^{n+\frac{1}{2}} \right\|^2. \quad (4.14)
\end{aligned}$$

Similarly,

$$\frac{\gamma}{\Delta t} \left(\nabla \cdot (\eta^{n+1} - \eta^n), \nabla \cdot \Phi_h^{n+\frac{1}{2}} \right) \leq \gamma \|\nabla \cdot \eta_t(t^{n+1})\|^2 + \gamma \int_{t^n}^{t^{n+1}} \|\nabla \cdot \eta_{tt}\|^2 dt + \frac{\gamma}{2} \left\| \nabla \cdot \Phi_h^{n+\frac{1}{2}} \right\|^2. \quad (4.15)$$

$$\begin{aligned}
\left(\frac{u^{n+1} - u^n}{\Delta t} - u_t(t^{n+\frac{1}{2}}), \Phi_h^{n+\frac{1}{2}} \right) &\leq \frac{1}{2} \left\| \frac{u^{n+1} - u^n}{\Delta t} - u_t(t^{n+\frac{1}{2}}) \right\|^2 + \frac{1}{2} \left\| \Phi_h^{n+\frac{1}{2}} \right\|^2 \\
&= \frac{(\Delta t)^3}{2560} \int_{t^n}^{t^{n+1}} \|u_{ttt}\|^2 dt + \frac{1}{2} \left\| \Phi_h^{n+\frac{1}{2}} \right\|^2 \quad (4.16)
\end{aligned}$$

$$v(\nabla u^{n+\frac{1}{2}} - \nabla u(t^{n+\frac{1}{2}}), \nabla \Phi_h^{n+\frac{1}{2}}) \leq 3v \left\| \nabla u^{n+\frac{v}{12}} - \nabla u(t^{n+\frac{1}{2}}) \right\|^2 + \frac{v^2}{2} \left\| \Phi_h^{n+\frac{1}{2}} \right\|^2 \quad (4.17)$$

$$= \frac{v(\Delta t)^3}{16} \int_{t^n}^{t^{n+1}} \|\nabla u_{tt}\|^2 dt + \frac{v}{12} \left\| \Phi_h^{n+\frac{1}{2}} \right\|^2 \quad (4.18)$$

For the pressure term, since $\Phi_h^{n+\frac{1}{2}} \in V_h$, for any $q_h \in Q_h$,

$$(p(t^{n+\frac{1}{2}}) - p_h^{n+1}, \nabla \cdot \Phi_h^{n+\frac{1}{2}}) = (p(t^{n+\frac{1}{2}}) - q_h, \nabla \cdot \Phi_h^{n+\frac{1}{2}}), \quad (4.19)$$

which implies

$$(p(t^{n+\frac{1}{2}}) - p_h^{n+1}, \nabla \cdot \Phi_h^{n+\frac{1}{2}}) \leq \frac{1}{2\gamma} \inf_{q_h \in Q_h} \left\| p(t^{n+\frac{1}{2}}) - q_h \right\|^2 + \frac{\gamma}{2} \left\| \nabla \cdot \Phi_h^{n+\frac{1}{2}} \right\|^2. \quad (4.20)$$

Utilizing (4.13)-(4.20) we now have

$$\begin{aligned}
& \frac{1}{2\Delta t} \left(\|\Phi_h^{n+1}\|^2 - \|\Phi_h^n\|^2 \right) + \frac{\gamma}{2\Delta t} \left(\|\nabla \cdot \Phi_h^{n+1}\|^2 - \|\nabla \cdot \Phi_h^n\|^2 \right) + \frac{5\nu}{6} \left\| \nabla \Phi_h^{n+\frac{1}{2}} \right\|^2 \\
& \leq 3\nu \left\| \nabla \eta^{n+\frac{1}{2}} \right\|^2 + \frac{\gamma}{\Delta t} \left\| \nabla \cdot \eta_t(t^{n+1}) \right\|^2 + \frac{\gamma}{\Delta t} \int_{t^n}^{t^{n+1}} \left\| \nabla \cdot \eta_{tt} \right\|^2 dt + \frac{1}{2\gamma} \inf_{q_h \in Q_h} \left\| p(t^{n+\frac{1}{2}}) - q_h \right\|^2 \\
& + C(1+\nu)\Delta t^3 \left(\int_{t^n}^{t^{n+1}} \|u_{ttt}\|^2 dt + \int_{t^n}^{t^{n+1}} \|\nabla u_{tt}\|^2 dt \right) + \frac{\nu^2+1}{2} \left\| \Phi_h^{n+\frac{1}{2}} \right\|^2 + \gamma \left\| \nabla \cdot \Phi_h^{n+\frac{1}{2}} \right\|^2 \\
& \quad + (w_h^{n+\frac{1}{2}} \times u_h^{n+\frac{1}{2}}, \Phi_h^{n+\frac{1}{2}}) - \left((\nabla \times u(t^{n+\frac{1}{2}})) \times u(t^{n+\frac{1}{2}}), \Phi_h^{n+\frac{1}{2}} \right) \\
& \quad \left\| \eta_t(t^{n+1}) \right\|^2 + \int_{t^n}^{t^{n+1}} \left\| \eta_{tt} \right\|^2 dt. \quad (4.21)
\end{aligned}$$

For the nonlinear terms we have

$$\begin{aligned}
& (w_h^{n+\frac{1}{2}} \times u_h^{n+\frac{1}{2}}, \Phi_h^{n+\frac{1}{2}}) - \left((\nabla \times u(t^{n+\frac{1}{2}})) \times u(t^{n+\frac{1}{2}}), \Phi_h^{n+\frac{1}{2}} \right) + \left((\nabla \times u^{n+\frac{1}{2}}) \times u^{n+\frac{1}{2}}, \Phi_h^{n+\frac{1}{2}} \right) \\
& \quad - \left((\nabla \times u^{n+\frac{1}{2}}) \times u^{n+\frac{1}{2}}, \Phi_h^{n+\frac{1}{2}} \right) \\
& = \left((w_h^{n+\frac{1}{2}} - \nabla \times u^{n+\frac{1}{2}}) \times u^{n+\frac{1}{2}}, \Phi_h^{n+\frac{1}{2}} \right) + \left(w_h^{n+\frac{1}{2}} \times (u_h^{n+\frac{1}{2}} - u^{n+\frac{1}{2}}), \Phi_h^{n+\frac{1}{2}} \right) \\
& \quad + \left((\nabla \times u^{n+\frac{1}{2}}) \times u^{n+\frac{1}{2}} - (\nabla \times u(t^{n+\frac{1}{2}})) \times u(t^{n+\frac{1}{2}}), \Phi_h^{n+\frac{1}{2}} \right) \\
& = \left((w_h^{n+\frac{1}{2}} - \nabla \times u^{n+\frac{1}{2}}) \times u^{n+\frac{1}{2}}, \Phi_h^{n+\frac{1}{2}} \right) - \left(w_h^{n+\frac{1}{2}} \times \eta^{n+\frac{1}{2}}, \Phi_h^{n+\frac{1}{2}} \right) \\
& \quad + \left((\nabla \times u^{n+\frac{1}{2}}) \times u^{n+\frac{1}{2}} - (\nabla \times u(t^{n+\frac{1}{2}})) \times u(t^{n+\frac{1}{2}}), \Phi_h^{n+\frac{1}{2}} \right) \quad (4.22)
\end{aligned}$$

We bound the second to last and last terms in (4.22) by

$$\begin{aligned}
(w_h^{n+\frac{1}{2}} \times \eta^{n+\frac{1}{2}}, \Phi_h^{n+\frac{1}{2}}) & \leq C \left\| w_h^{n+\frac{1}{2}} \right\| \left\| \nabla \eta^{n+\frac{1}{2}} \right\| \left\| \nabla \Phi_h^{n+\frac{1}{2}} \right\| \\
& \leq \frac{\nu}{12} \left\| \nabla \Phi_h^{n+\frac{1}{2}} \right\|^2 + 3\nu^{-1} \left\| w_h^{n+\frac{1}{2}} \right\|^2 \left\| \nabla \eta^{n+\frac{1}{2}} \right\|^2 \quad (4.23)
\end{aligned}$$

$$\begin{aligned}
& (u(t^{n+\frac{1}{2}}) \times (\nabla \times u(t^{n+\frac{1}{2}})) - u^{n+\frac{1}{2}} \times (\nabla \times u^{n+\frac{1}{2}}), \Phi_h^{n+\frac{1}{2}}) \\
& \leq \frac{\nu}{12} \left\| \nabla \Phi_h^{n+\frac{1}{2}} \right\|^2 + 3\nu^{-1} \left\| u(t^{n+\frac{1}{2}}) \times (\nabla \times u(t^{n+\frac{1}{2}})) - u^{n+\frac{1}{2}} \times (\nabla \times u^{n+\frac{1}{2}}) \right\|^2 \\
& \leq \frac{\nu}{12} \left\| \nabla \Phi_h^{n+\frac{1}{2}} \right\|^2 + \frac{3}{48} \nu^{-1} (\Delta t)^3 \int_{t^n}^{t^{n+1}} \left\| (u \times (\nabla \times u))_{tt} \right\|^2 dt. \quad (4.24)
\end{aligned}$$

For the first term in (4.22), we first need a bound on $\left\| \nabla \times u^{n+\frac{1}{2}} - w_h^{n+\frac{1}{2}} \right\|$. This is obtained by restricting χ_h to V_h in (2.6) and then subtracting $(\nabla \times u^{n+\frac{1}{2}}, \chi_h)$ from both sides of (2.6), which gives us

$$\begin{aligned} (\nabla \times u^{n+\frac{1}{2}} - w_h^{n+\frac{1}{2}}, \chi_h) &= (\nabla \times (u^{n+\frac{1}{2}} - u_h^{n+\frac{1}{2}}), \chi_h) \\ &= (\nabla \times \eta^{n+\frac{1}{2}}, \chi_h) + (\nabla \times \Phi_h^{n+\frac{1}{2}}, \chi_h). \end{aligned}$$

By the definition of P_{V_h} ,

$$\begin{aligned} (P_{V_h}(\nabla \times u^{n+\frac{1}{2}}) - w_h^{n+\frac{1}{2}}, \chi_h) &= (\nabla \times u^{n+\frac{1}{2}} - w_h^{n+\frac{1}{2}}, \chi_h) \\ &= (\nabla \times (u^{n+\frac{1}{2}} - u_h^{n+\frac{1}{2}}), \chi_h) \\ &= (\nabla \times \eta^{n+\frac{1}{2}}, \chi_h) + (\nabla \times \Phi_h^{n+\frac{1}{2}}, \chi_h) \end{aligned}$$

Choose $\chi_h = P_{V_h}(\nabla \times u^{n+\frac{1}{2}}) - w_h^{n+\frac{1}{2}}$ we obtain

$$\left\| P_{V_h}(\nabla \times u^{n+\frac{1}{2}}) - w_h^{n+\frac{1}{2}} \right\|^2 \leq 2 \left(\left\| \nabla \eta^{n+\frac{1}{2}} \right\|^2 + \left\| \nabla \Phi_h^{n+\frac{1}{2}} \right\|^2 \right). \quad (4.25)$$

Now using (4.25) and, from Poincaré's inequality, $\left\| \Phi_h^{n+\frac{1}{2}} \right\| \leq C \left\| \nabla \Phi_h^{n+\frac{1}{2}} \right\|$ we obtain

$$\begin{aligned} &\left((P_{V_h}(\nabla \times u^{n+\frac{1}{2}}) - w_h^{n+\frac{1}{2}}) \times u^{n+\frac{1}{2}}, \Phi_h^{n+\frac{1}{2}} \right) \\ &\leq C \left\| \nabla u^{n+\frac{1}{2}} \right\| \left\| P_{V_h}(\nabla \times u^{n+\frac{1}{2}}) - w_h^{n+\frac{1}{2}} \right\| \left\| \Phi_h^{n+\frac{1}{2}} \right\|^{\frac{1}{2}} \left\| \nabla \Phi_h^{n+\frac{1}{2}} \right\|^{\frac{1}{2}} \\ &\leq C \left\| \nabla u^{n+\frac{1}{2}} \right\| \left(\left\| \nabla \eta^{n+\frac{1}{2}} \right\| \left\| \nabla \Phi_h^{n+\frac{1}{2}} \right\| + \left\| \Phi_h^{n+\frac{1}{2}} \right\|^{\frac{1}{2}} \left\| \nabla \Phi_h^{n+\frac{1}{2}} \right\|^{\frac{3}{2}} \right) \\ &\leq \frac{\nu}{12} \left\| \nabla \Phi_h^{n+\frac{1}{2}} \right\|^2 + C\nu^{-1} \left\| \nabla u^{n+\frac{1}{2}} \right\|^2 \left\| \nabla \eta^{n+\frac{1}{2}} \right\|^2 + \frac{\nu}{12} \left\| \nabla \Phi_h^{n+\frac{1}{2}} \right\|^2 + C\nu^{-3} \left\| \nabla u^{n+\frac{1}{2}} \right\|^4 \left\| \Phi_h^{n+\frac{1}{2}} \right\|^2. \end{aligned} \quad (4.26)$$

Also, we have that

$$\begin{aligned} &\left((\nabla \times u^{n+\frac{1}{2}} - P_{V_h}(\nabla \times u^{n+\frac{1}{2}})) \times u^{n+\frac{1}{2}}, \Phi_h^{n+\frac{1}{2}} \right) \\ &\leq C \left\| \nabla \times u^{n+\frac{1}{2}} - P_{V_h}(\nabla \times u^{n+\frac{1}{2}}) \right\| \left\| \nabla u^{n+\frac{1}{2}} \right\| \left\| \nabla \Phi_h^{n+\frac{1}{2}} \right\| \\ &\leq \frac{\nu}{12} \left\| \nabla \Phi_h^{n+\frac{1}{2}} \right\|^2 + C \left\| \nabla u^{n+\frac{1}{2}} \right\|^2 \left\| \nabla \times u^{n+\frac{1}{2}} - P_{V_h}(\nabla \times u^{n+\frac{1}{2}}) \right\|^2 \end{aligned} \quad (4.27)$$

We combine the estimates (4.27) and (4.26) and obtain the desired bound for the term $\left((w_h^{n+\frac{1}{2}} - \nabla \times u^{n+\frac{1}{2}}) \times u^{n+\frac{1}{2}}, \Phi_h^{n+\frac{1}{2}} \right)$.

Noting that $\left\| \nabla \cdot \Phi_h^{n+\frac{1}{2}} \right\|^2 \leq 1/2 (\|\nabla \cdot \Phi_h^{n+1}\|^2 + \|\nabla \cdot \Phi_h^n\|^2)$, substituting the bounds derived in (4.23), (4.24), (4.26), and (4.27) into (4.21) yields

$$\begin{aligned}
& \frac{1}{2\Delta t} \left(\|\Phi_h^{n+1}\|^2 - \|\Phi_h^n\|^2 \right) + \frac{\gamma}{2\Delta t} \left(\|\nabla \cdot \Phi_h^{n+1}\|^2 - \|\nabla \cdot \Phi_h^n\|^2 \right) + \frac{\nu}{2} \left\| \nabla \Phi_h^{n+\frac{1}{2}} \right\|^2 \\
& \leq \left(\frac{\nu^2 + 4}{2} + C\nu^{-3} \left\| \nabla u^{n+\frac{1}{2}} \right\|^4 \right) \left\| \Phi_h^{n+\frac{1}{2}} \right\|^2 + \frac{\gamma}{2} \left(\|\nabla \cdot \Phi_h^{n+1}\|^2 + \|\nabla \cdot \Phi_h^n\|^2 \right) \\
& + \frac{1}{2\gamma} \inf_{q_h \in Q_h} \|p(t^{n+1}) - q_h\|^2 + C\nu \left\| \nabla \eta^{n+\frac{1}{2}} \right\|^2 + \|\eta_t(t^{n+1})\|^2 + \gamma \|\nabla \cdot \eta_t(t^{n+1})\|^2 \\
& + C\nu^{-1} \left\| w_h^{n+\frac{1}{2}} \right\|^2 \left\| \nabla \eta^{n+\frac{1}{2}} \right\|^2 + \nu^{-1} \left\| \nabla u^{n+\frac{1}{2}} \right\|^2 \left\| \nabla \eta^{n+\frac{1}{2}} \right\|^2 + \int_{t^n}^{t^{n+1}} \|\eta_{tt}\|^2 dt \\
& + \gamma \int_{t^n}^{t^{n+1}} \|\nabla \cdot \eta_{tt}\|^2 dt + C\Delta t^3 \left(\int_{t^n}^{t^{n+1}} \|u_{ttt}\|^2 dt + \int_{t^n}^{t^{n+1}} \|\nabla u_{tt}\|^2 dt \right) \\
& + C\nu^{-1} (\Delta t)^3 \int_{t^n}^{t^{n+1}} \|(u \times (\nabla \times u))_{tt}\|^2 dt + C \left\| \nabla u^{n+\frac{1}{2}} \right\|^2 \left\| \nabla \times u^{n+\frac{1}{2}} - P_{V_h}(\nabla \times u^{n+\frac{1}{2}}) \right\|^2
\end{aligned} \tag{4.28}$$

Next multiply by $2\Delta t$, sum over time steps, and using the Gronwall inequality (from [11]) yields

$$\begin{aligned}
& \left\| \Phi_h^M \right\|^2 + \gamma \|\nabla \cdot \Phi_h^M\|^2 + \nu \Delta t \sum_{n=0}^{M-1} \left\| \nabla \Phi_h^{n+\frac{1}{2}} \right\|^2 \\
& \leq C \exp \left(2\Delta t \sum_{n=0}^{M-1} \gamma + \frac{\nu^2 + 4}{2} + C\nu^{-3} \left\| \nabla u^{n+\frac{1}{2}} \right\|^4 \right) \left(\Delta t \sum_{n=1}^M \frac{1}{2\gamma} \inf_{q_h \in Q_h} \|p(t^n) - q_h\|^2 \right. \\
& + \Delta t \sum_{n=0}^M \nu \|\nabla \eta^n\|^2 + \Delta t \sum_{n=1}^M \|\eta_t(t^n)\|^2 + \Delta t \sum_{n=1}^M \gamma \|\nabla \eta_t(t^n)\|^2 + \Delta t \sum_{n=0}^{M-1} \nu^{-1} \left\| w_h^{n+\frac{1}{2}} \right\|^2 \left\| \nabla \eta^{n+\frac{1}{2}} \right\|^2 \\
& + \Delta t \sum_{n=0}^{M-1} \nu^{-1} \left\| \nabla u^{n+\frac{1}{2}} \right\|^2 \left\| \nabla \eta^{n+\frac{1}{2}} \right\|^2 + \Delta t \sum_{n=0}^{M-1} \int_{t^n}^{t^{n+1}} \|\eta_{tt}\|^2 dt \\
& + \Delta t \sum_{n=0}^{M-1} \gamma \int_{t^n}^{t^{n+1}} \|\nabla \cdot \eta_{tt}\|^2 dt + (\Delta t)^4 \|u_{ttt}\|_{2,0}^2 + (\Delta t)^4 \|\nabla u_{tt}\|_{2,0}^2 + (\Delta t)^4 \|(u \times (\nabla \times u))_{tt}\|_{2,0}^2 \\
& \left. + \Delta t \sum_{n=0}^{M-1} \left\| \nabla u^{n+\frac{1}{2}} \right\|^2 \left\| \nabla \times u^{n+\frac{1}{2}} - P_{V_h}(\nabla \times u^{n+\frac{1}{2}}) \right\|^2 \right) \tag{4.29}
\end{aligned}$$

Recall the approximation properties of $U^n \in V_h$, $q_h \in Q_h$, and P_{V_h} [13]

$$\begin{aligned} \|\eta(t^n)\|_s &\leq Ch^{k+1-s} \|u(t^n)\|_{k+1}, \quad s = 0, 1, \quad \text{and} \\ \inf_{q_h \in Q_h} \|p(t^n) - q_h\| &\leq Ch^k \|p(t^n)\|_k \\ \|w^n - P_{V_h}(w^n)\| &\leq Ch^{k+1} \|w^n\|_{k+1}. \end{aligned}$$

Estimate (4.29) then becomes

$$\begin{aligned} &\|\Phi_h^M\|^2 + \gamma \|\nabla \cdot \Phi_h^M\|^2 + \nu \Delta t \sum_{n=0}^{M-1} \left\| \nabla \Phi_h^{n+\frac{1}{2}} \right\|^2 \\ &\leq C \exp \left(2\Delta t \sum_{n=0}^{M-1} \gamma + \frac{\nu^2 + 4}{2} + C\nu^{-3} \left\| \nabla u^{n+\frac{1}{2}} \right\|^4 \right) \left(\frac{1}{2\gamma} h^{2k} \|p\|_{2,k}^2 \right. \\ &\quad + \nu h^{2k} \|u\|_{2,k+1}^2 + h^{2k+2} \|u_t\|_{2,k+1}^2 + \gamma h^{2k} \|u_t\|_{2,k+1}^2 \\ &\quad + \nu^{-1} h^{2k} \|u_t\|_{\infty,1}^2 \|u\|_{2,k+1}^2 + \Delta t \gamma h^{2k} \|u_{tt}\|_{2,k+1}^2 + \Delta t h^{2k+2} \|u_{tt}\|_{2,k+1}^2 \\ &\quad + (\Delta t)^4 \|u_{ttt}\|_{2,0}^2 + (\Delta t)^4 \|\nabla u_{tt}\|_{2,0}^2 + (\Delta t)^4 \|(u \times (\nabla \times u))_{tt}\|_{2,0}^2 \\ &\quad \left. + \left(\nu \Delta t \sum_{n=0}^{M-1} \left\| w_h^{n+\frac{1}{2}} \right\|^2 \right) \nu^{-2} h^{2k} \|u_t\|_{\infty,k+1}^2 + h^{2k+2} \|u\|_{\infty,1}^2 \|\nabla \times u\|_{2,k+1}^2 \right) \quad (4.30) \end{aligned}$$

Finally, from the boundness estimate for $\nu \Delta t \sum_{n=0}^{M-1} \left\| w_h^{n+\frac{1}{2}} \right\|^2$ from (3.4), and an application of the triangle inequality we obtain (4.7). □

Remark 4.1. As expected, if (X_h, Q_h) is chosen to be the inf-sup stable pair (P_k, P_{k-1}) , $k \geq 2$, then with the smoothness assumptions (4.1)-(4.6) and $p \in L^2(0, T; H^k(\Omega))$ the H^1 convergence for the velocity is

$$\|u - u_h\|_{2,1} \leq C(\Delta t^2 + h^k) \quad (4.31)$$

Remark 4.2. The significant computational improvement of Schemes 2 and 3 over Scheme 1 is somewhat masked in the statement of the a priori error bound for the velocity (for Scheme 3) given in (4.7). For Scheme 1 the pressure contribution to the bound is $C/\nu \|p - q_h\|$, whereas for Schemes 2 and 3 the pressure contribution is given by $C\|p - q_h\|$, see (4.20). The presence of ν in the denominator for Scheme 1 suggests a superior numerical performance of Schemes 2 and 3 if a large pressure error is present.

5 Numerical Experiments

This section presents two numerical experiments, the first to confirm convergence rates and the second to compare the schemes' accuracies over a longer time interval, against

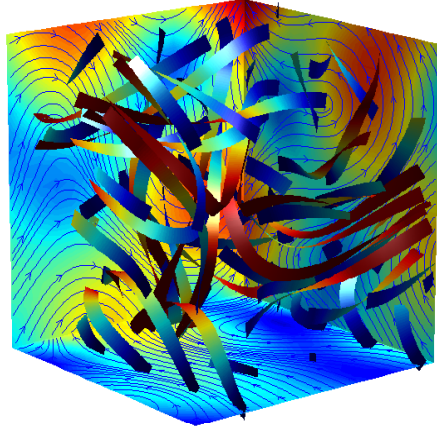


Figure 1: The velocity solution to the Ethier-Steinman problem with $a = 1.25$, $d = 1$ at $t = 0$ on the $(-1, 1)^3$ domain. The complex flow structure is seen in the streamribbons in the box and the velocity streamlines and speed contours on the sides.

each other and a commonly used scheme. For both experiments, we will compute approximations to the Ethier-Steinman exact Navier-Stokes solution on $[-1, 1]^3$ [7], although we choose different parameters and viscosities for the two tests. We find in the first numerical experiment, computed convergence rates from successive mesh and time-step refinements indeed match the predicted rates from section 4. For the second experiment, the advantage of using the stabilized enhanced physics based scheme is demonstrated.

For chosen parameters a, d and viscosity ν , the exact Ethier-Steinman NSE solution is given by

$$u_1 = -a(e^{ax} \sin(ay + dz) + e^{az} \cos(ax + dy)) e^{-\nu d^2 t} \quad (5.1)$$

$$u_2 = -a(e^{ay} \sin(az + dx) + e^{ax} \cos(ay + dz)) e^{-\nu d^2 t} \quad (5.2)$$

$$u_3 = -a(e^{az} \sin(ax + dy) + e^{ay} \cos(az + dx)) e^{-\nu d^2 t} \quad (5.3)$$

$$\begin{aligned} p = & -\frac{a^2}{2}(e^{2ax} + e^{2ay} + e^{2az} + 2 \sin(ax + dy) \cos(az + dx) e^{a(y+z)} \\ & + 2 \sin(ay + dz) \cos(ax + dy) e^{a(z+x)} \\ & + 2 \sin(az + dx) \cos(ay + dz) e^{a(x+y)}) e^{-2\nu d^2 t} \end{aligned} \quad (5.4)$$

We give the pressure in its usual form, although our scheme approximates instead the Bernoulli pressure $P = p + \frac{1}{2} |u|^2$. This problem was developed as a 3d analogue to the Taylor vortex problem, for the purpose of benchmarking. Although unlikely to be physically realized, it is a good test problem because it is not only an exact NSE solution, but also it has non-trivial helicity which implies the existence of complex structure [18] in the velocity field. The $t = 0$ solution for $a = 1.25$ and $d = 1$ is illustrated in Figure 1. For both experiments below, we use $u^0 = (u_1(0), u_2(0), u_3(0))^T$ as the initial condition

and enforce Dirichlet boundary conditions for velocity to be the interpolant of $u(t)$ on the boundary, while a do-nothing boundary condition is used for the vorticity projection. All computations with schemes 2 and 3 use stabilization parameter $\gamma = 1$.

5.1 Numerical Test 1: Convergence rate verification

h	Δt	$\ u - u_{S1}\ _{2,1}$	rate	$\ u - u_{S2}\ _{2,1}$	rate	$\ u - u_{S3}\ _{2,1}$	rate
1	0.001	0.01560	-	0.01556	-	0.01579	-
0.5	0.0005	0.00390	2.00	0.00391	1.99	0.00395	2.00
0.25	0.00025	0.000979	1.99	0.000979	2.00	0.000984	2.01
0.125	0.000125	0.000245	2.00	0.000245	2.00	0.000246	2.00

Table 1: The $\|u_{NSE} - u_h\|_{2,1}$ errors and convergence rates for each of the three scheme of algorithm 2.1.

To verify convergence rates predicted in section 4, we compute approximations to (5.1)-(5.4) with parameters $a = d = \pi/4$, viscosity $\nu = 1$, and end-time $T = 0.001$. Since (P_2, P_1) elements are being used, we expect $O(h^2 + \Delta t^2)$ convergence of $\|u_{NSE} - u_h\|_{2,1}$ for each of the three schemes of Algorithm 2.1. Errors and rates in this norm are shown in table 1, and we find they match those predicted by the theory.

5.2 Numerical Test 2: Comparison of the schemes

For our second test, we compute approximations to (5.1)-(5.4) with $a = 1.25$, $d = 1$, kinematic viscosity $\nu = 0.002$, end time $T = 0.5$, using all 3 schemes from Algorithm 2.1. We use 3,072 tetrahedral elements, which provides 41,472 velocity degrees of freedom, and 46,875 degrees of freedom for the projected vorticity since here there are degrees of freedom on the boundary. It is important to note that due to the splitting of the projection equations from the NSE system in the solver and since the projection equation is well-conditioned, the time spent for assembling and solving the projection equations is negligible.

In addition to the 3 schemes of Algorithm 2.1, for comparison, we also compute approximations using the well-known convective form Crank-Nicolson (CCN) FEM for the Navier-Stokes equations [13, 10, 12]. We run the simulations with time-step $\Delta t = 0.005$. Results of the simulations are shown in figures 2 and 3, where $L^2(\Omega)$ error and helicity error are plotted against time. Is clear from the pictures that the enhanced physics based scheme is superior to the usual Crank-Nicolson scheme, and its advantage becomes more pronounced with larger time. Also it is seen how the stabilizations of the enhanced-physics scheme improve accuracy.

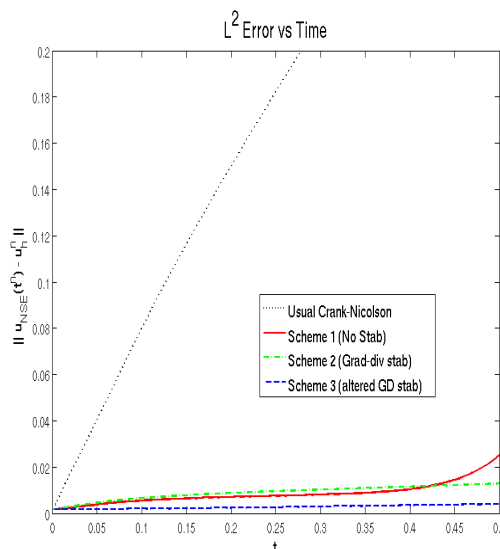


Figure 2: The plot above shows L_2 error of the velocity vs time for the four schemes of test 2. We see in the plot that the stabilizations add accuracy to the enhanced-physics scheme, and that the altered grad-div stabilization gives slightly better results than the usual grad-div stabilization. It can also be seen that the enhanced-physics scheme is far more accurate in this metric than the usual Crank-Nicolson scheme.

6 Conclusions and future directions

We have extended the methodology of the enhanced-physics based scheme of [23] to a more general set of problems. This extension required the use of grad-div type stabilizations since the scheme uses a Bernoulli pressure which can be a dominant source of error in finite element computations, and we proposed an altered grad-div stabilization that appears to stabilize in a similar way as the usual grad-div stabilization, but provides a more physical solution by not altering the energy balance. We also provided a numerical example that showed the advantage of the enhanced physics based scheme as well as for the altered grad-div stabilization that we use.

As discussed in the Introduction, with the rotational form of the NSE and introduction of the Bernoulli pressure, the pressure term in the a priori error estimate for the velocity approximation can have a significant impact. An alternative to a grad-div stabilization method may be to choose the approximation spaces (X_h, Q_h) so that the pressure term does not appear in the a priori error estimate for the velocity approximation. Recently stable approximation spaces (X_h, Q_h) , Scott-Vogelius elements [28] (see [27, 26, 24, 25] for $\Omega \subset \mathbb{R}^2$), have been introduced for which $[\nabla \cdot X_h] \subset Q_h$, which guarantees that discretely divergence free approximations for the velocity are also L^2 divergence free. These elements require a special mesh, and are higher order (at least) $P_3(e) - (\text{discontinuous})P_2(e)$ compared to the commonly used Taylor-Hood elements $P_2(e) - P_1(e)$. Future work will include a comparison of the stabilized methods investi-

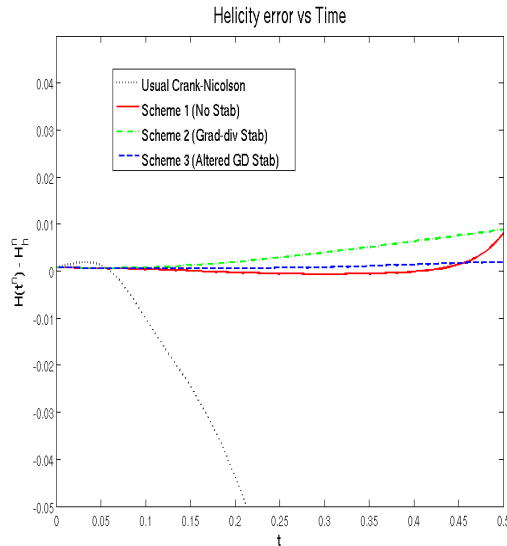


Figure 3: The plot above shows helicity error vs time for the four schemes of test 2. We see in the plot that helicity is far more accurate in the enhanced-physics scheme, and even better with stabilizations, than the usual Crank-Nicolson scheme.

gated above with approximations using Scott-Vogelius elements.

References

- [1] A. Arakawa. Computational design for long-term numerical integration of the equations of fluid motion: Two dimensional incompressible flow, Part I. *J. Comput. Phys.*, 1:119–143, 1966.
- [2] A. Arakawa and V. Lamb. A potential enstrophy and energy conserving scheme for the shallow water equations. *Monthly Weather Review*, 109:18–36, 1981.
- [3] Q. Chen, S. Chen, and G. Eyink. The joint cascade of energy and helicity in three dimensional turbulence. *Physics of Fluids*, 15(2):361–374, 2003.
- [4] J. Conners. Convergence analysis and computational testing of the finite element discretization of the Navier-Stokes-alpha model. *Submitted*, 2009.
- [5] P. Ditlevson and P. Guiliani. Cascades in helical turbulence. *Physical Review E*, 63, 2001.
- [6] V.J. Ervin and N. Heuer. Approximation of time-dependent, viscoelastic fluid flow: Crank-Nicolson, finite element approximation. *Numer. Methods Partial Differential Eq.*, 20:248–283, 2003.

- [7] C. Ethier and D. Steinman. Exact fully 3d Navier-Stokes solutions for benchmarking. *International Journal for Numerical Methods in Fluids*, 19(5):369–375, 1994.
- [8] M. Gavrilov and Z. Janji. Computed rotational energy spectra of two energy and enstrophy conserving schemes on semi-staggered grids. *Meteorology and Atmospheric Physics*, 41(1):1–4, 1989.
- [9] V. Girault and P.-A. Raviart. *Finite element methods for Navier-Stokes equations : Theory and algorithms*. Springer-Verlag, 1986.
- [10] M. Gunzburger. *Finite Element Methods for Viscous Incompressible Flow: A Guide to Theory, Practice, and Algorithms*. Academic Press, Boston, 1989.
- [11] J. Heywood and R. Rannacher. Finite element approximation of the nonstationary Navier-Stokes problem. Part IV: Error analysis for the second order time discretization. *SIAM J. Numer. Anal.*, 2:353–384, 1990.
- [12] V. John. *Large Eddy Simulation of Turbulent Incompressible Flows. Analytical and Numerical Results for a Class of LES Models*, volume 34 of *Lecture Notes in Computational Science and Engineering*. Springer-Verlag Berlin, Heidelberg, New York, 2004.
- [13] W. Layton. *An introduction to the numerical analysis of viscous incompressible flows*. SIAM, 2008.
- [14] W. Layton, C. Manica, M. Neda, M.A. Olshanskii, and L. Rebholz. On the accuracy of the rotation form in simulations of the Navier-Stokes equations. *J. Comput. Phys.*, 228(5):3433–3447, 2009.
- [15] A. Linke. *Divergence-free mixed finite elements for the incompressible Navier-Stokes Equation*. PhD thesis, University of Erlangen, 2007.
- [16] J. Liu and W. Wang. Energy and helicity preserving schemes for hydro and magnetohydro-dynamics flows with symmetry. *J. Comput. Phys.*, 200:8–33, 2004.
- [17] C. Manica, M. Neda, M. Olshanskii, and L. Rebholz. Enabling accuracy of Navier-Stokes-alpha through deconvolution and enhanced stability. *Submitted*, 2009.
- [18] H. Moffatt and A. Tsoniber. Helicity in laminar and turbulent flow. *Annual Review of Fluid Mechanics*, 24:281–312, 1992.
- [19] I.M Navon. Implementation of a posteriori methods for enforcing conservation of potential enstrophy and mass in discretized shallow water equation models. *Monthly Weather Review*, 109:946–958, 1981.
- [20] I.M. Navon. A Numerov-Galerkin technique applied to a finite element shallow water equations model with enforced conservation of integral invariants and selective lumping. *J. Comput. Phys.*, 52:313–339, 1983.

- [21] M. Olshanskii, G. Lube, T. Heister, and J. Löwe. Grad-div stabilization and subgrid pressure models for the incompressible Navier-Stokes equations. *Comp. Meth. Appl. Mech. Eng.*, 2009, to appear.
- [22] M.A. Olshanskii and A. Reusken. Grad-Div stabilization for the Stokes equations. *Math. Comp.*, 73:1699–1718, 2004.
- [23] L. Rebholz. An energy and helicity conserving finite element scheme for the Navier-Stokes equations. *SIAM Journal on Numerical Analysis*, 45(4):1622–1638, 2007.
- [24] L.R. Scott and M. Vogelius. Conforming finite element methods for incompressible and nearly incompressible continua. In *Large-scale computations in fluid mechanics, Part 2*, volume 22-2 of *Lectures in Applied Mathematics*, pages 221–244. Amer. Math. Soc., 1985.
- [25] L.R. Scott and M. Vogelius. Norm estimates for a maximal right inverse of the divergence operator in spaces of piecewise polynomials. *Mathematical Modelling and Numerical Analysis*, 19(1):111–143, 1985.
- [26] M. Vogelius. An analysis of the p -version of the finite element method for nearly incompressible materials. uniformly valid, optimal error estimates. *Numer. Math.*, 41:39–53, 1983.
- [27] M. Vogelius. A right-inverse for the divergence operator in spaces of piecewise polynomials. Application to the p -version of the finite element method. *Numer. Math.*, 41:19–37, 1983.
- [28] S. Zhang. A new family of stable mixed finite elements for the 3d Stokes equations. *Math. Comp.*, 74(250):543–554, 2005.